AD_____

Award Number: W81XWH-10-1-0702

TITLE: Promoting Cartilage Stem Cell Activity to Improve Recovery from Joint Fracture

PRINCIPAL INVESTIGATOR: James A. Martin, PhD

CONTRACTING ORGANIZATION: University of Iowa
Iowa City, Iowa 522452-1100

REPORT DATE: September 2012

TYPE OF REPORT: Final

PREPARED FOR: U.S. Army Medical Research and Materiel Command
Fort Detrick, Maryland 21702-5012

REPORT DOCUMENTATION PAGE

Form Approved
OMB No. 0704-0188

1. REPORT DATE *(DD-MM-YYYY)*	2. REPORT TYPE	3. DATES COVERED *(From - To)*
September 2012	Final	27 September 2010 - 26 August 2012

4. TITLE AND SUBTITLE
Promoting Cartilage Stem Cell Activity to Improve Recovery from Joint Fracture

Fracture

5a. CONTRACT NUMBER

5b. GRANT NUMBER
W81XWH-10-1-0702

5c. PROGRAM ELEMENT NUMBER

6. AUTHOR(S)
James A. Martin, PhD[1]

5d. PROJECT NUMBER

5e. TASK NUMBER

5f. WORK UNIT NUMBER

7. PERFORMING ORGANIZATION NAME(S) AND ADDRESS(ES)
University of Iowa
Iowa City, Iowa 522452-1100

8. PERFORMING ORGANIZATION REPORT NUMBER

9. SPONSORING / MONITORING AGENCY NAME(S) AND ADDRESS(ES)
U.S. Army Medical Research and Materiel Command, Fort Detrick, Maryland 21702-5012

10. SPONSOR/MONITOR'S ACRONYM(S)

11. SPONSOR/MONITOR'S REPORT NUMBER(S)

12. DISTRIBUTION / AVAILABILITY STATEMENT
Approved for public release; distribution unlimited

13. SUPPLEMENTARY NOTES

14. ABSTRACT

It has been assumed that chondrocytes killed by mechanical injury to articular cartilage are never replaced and that the resulting hypocellularity contributes to post-traumatic osteoarthritis. However, we found that nonviable areas in an explant injury model were repopulated within 7-14 days by cells that appeared to migrate from the surrounding matrix. We hypothesized that the migrating population included chondrogenic progenitor cells drawn to injured cartilage by alarmins released from dead chondrocytes.

Injuries that caused chondrocyte death stimulated the emergence and homing of chondrogenic progenitors via RAGE-mediated chemotaxis. Moreover, when supplied with a fibrin matrix chondrogenic progenitor cells regenerated cartilage in a chondral defect. Thus, we confirmed an endogenous mechanism that may be leveraged to repair cartilage defects in vivo that might otherwise lead to progressive cartilage loss.

15. SUBJECT TERMS
Chondrogenic progenitor cells, chemotaxis, cartilage repair

16. SECURITY CLASSIFICATION OF:			17. LIMITATION OF ABSTRACT	18. NUMBER OF PAGES	19a. NAME OF RESPONSIBLE PERSON
a. REPORT	b. ABSTRACT	c. THIS PAGE			USAMRMC
U	U	U	UU	12	19b. TELEPHONE NUMBER *(include area code)*

Standard Form 298 (Rev. 8-98)
Prescribed by ANSI Std. Z39.18

111

Table of Contents

Page

INTRODUCTION:

This proposal is concerned with enhancing the environment for cartilage healing following intra-articular fractures (IAFs). Chondrocyte mortality resulting from high energy injuries that lead to IAFs is a significant barrier to the restoration of joint surfaces [1-3]. Although therapies that maintain or restore normal cellularity have shown promise *in vitro* models, few have been tested *in vivo* and none are yet available for use in patients. Recent work confirms earlier observations, which revealed migratory cells on cartilage surfaces in explant culture [9,10]. Real-time confocal imaging of blunt impact-injured cartilage showed that dead zones in the matrix could be repopulated by stem cell-like cells that appear to infiltrate from nearby cartilage. This unforeseen result raises the possibility that a cell-based regenerative mechanism is at work in injured cartilage. If so, harnessing it's potential offers enormous promise as a simple, safe, and effective means to reverse early cartilage damage. It is expected that the knowledge gained by this effort will help to identify methods to restore cellularity in injured cartilage that are most likely to be effective under physiologic conditions and therefore merit further testing *in vivo* in the survival animal model currently under development.

BODY:

We originally planned to in Specific Aim 1 to evaluate the effects of cell death inhibitors and the occurrence of migrating cells in an ex vivo fracture model. However, it soon became apparent that chondrocyte death itself whether caused by fracture or direct cartilage impact was the key factor in activating the cells to migrate. Thus, we focused on our osteochondral explant impact model, which made it much easier to elucidate molecular and cellular aspects of activation and to determine the identity and repair potential of the migrating population. The following is a summary of our findings relevant to tasks outlined for Specific Aims 2 and 3.

Chondrogenic Progenitor Cells Respond to Cartilage Injury

Background

A number of studies have shown that blunt trauma to articular cartilage of the kind seen in many joint injuries induces acute chondrocyte necrosis and apoptosis (36-42). These losses in cellularity have been thought to be irreversible (1, 36). However, in an explant trauma model we found that devitalized zones were frequently re-populated over a period of 5-12 days post-impact by cells that appeared to migrate over the cartilage surface into the injury site. We hypothesized that these were CPCs responding to alarmins released by dead chondrocytes. To test this, we isolated surface-adherent migrating cells and determined their ability to move toward injured cartilage. The *in vitro* chemotactic activity, clonality, and multi-potency of the putative CPCs (pCPCs) were compared with normal chondrocytes (NCs). Gene expression profiling was used to assess the phenotypic relatedness of migrating cells to normal chondrocytes and marrow stromal cells (MSCs). Hoechst dye exclusion assays were performed to measure the percentage of stem-like cells in each population. Chemotaxis/invasion assays were used to measure the response to chemokines, dead cell debris and purified HMGB1.

Materials and Methods

Bovine stifle joints from skeletally mature animals were obtained after slaughter from a local abattoir (Bud's Custom Meats, Riverside, IA). Osteochondral explants were prepared by manually sawing an approximately 25 x 25 mm^2 from bovine tibial plateau, which included the central loaded area of the articular surface. The explants were rinsed in Hanks Balances Salt Solution (HBSS) and cultured in Dulbecco's modified Eagle medium (DMEM) supplemented with 10% fetal bovine serum (Invitrogen, Carlsbad, CA), 50 μg/ml L-ascorbate, 100 U/ml penicillin, 100 μg/ml streptomycin, and 2.5 μg/ml Fungizone.

After two days in culture the explants were injured by blunt impact (14 J/cm^2) *via* a 5 mm-diameter flat-ended platen using a drop tower device as described previously (42, 43). Confocal imaging studies were performed essentially as described (42, 43). Briefly, explants were stained with calcein AM (viability) and ethidium homodimer (dead cells) and submerged in culture medium in a specimen cup. After a 30-minute incubation, specimen cups were placed in the custom-built x-y microscope stage driver (CMSD), which as mounted on a Bio-Rad 1024 laser scanning confocal microscope (LSCM) (Bio-Rad Laboratories Inc., Hercules, CA). An etched glass target reticle within the CMSD device was used for accurate and precise alignment of the tissue with the microscope. This system enabled repeated imaging of the same sites to observe migrating cell infiltration. Each site was imaged in z-series (every 20 microns to an average depth of approximately 200 microns). Specimens were placed in fresh culture medium after each imaging session and were re-stained before each imaging session.

Five to seven days post-injury explant surfaces were submerged in 0.25% trypsin-EDTA in HBSS and were incubated for 10 minutes to detach migrating progenitor cells from the surface. Pre-and post-trypsin imaging studies confirmed that the brief enzymatic treatment removed the surface-adherent migrating cells without disrupting the underlying superficial chondrocytes. To recover normal chondrocytes the underlying

cartilage was digested overnight with collagenase type 1 and pronase E (Sigma-Aldrich, St. Louis, MO) dissolved in culture medium (0.25 mg/ml each).

For some experiments isolated pCPCs cells were labeled with Green Fluorescent Protein (GFP, 488 nm) by lentiviral transduction. The transduction efficiency reached approximately 40%. GFP-labeled cells ($1x10^5$) were suspended in a chilled (8°C) temperature-sensitive hydrogel (0.6% hyaluronic acid, 18% F-127). The suspension was overlain on explant surfaces adjacent to a blunt impact site. The gel solidified upon contact with the warm explants such that the suspended cells were held in place. The explants were incubated for 5 days when they were counterstained with 0.5 μM Cell Tracker Red CMTPX (Invitrogen, Carlsbad, CA) and imaged on a Bio-Rad 1024 confocal microscope with the CMSD. The sites were scanned to an average depth of 330 μm at 40 μm intervals. Z-axis projections of confocal images were made using ImageJ (rsb.info.nih.gov/ij).

For colony forming assays 200 pCPCs or normal chondrocytes from the superficial 1/3 or lower 2/3 of the matrix were plated in 150-mm culture dishes and incubated for 10 days. A custom-fabricated device was used to separate the cartilage zones prior to collagenase/pronase digestion. The colonies were fixed in 10% neutral-buffered formalin and visualized by Richardson's stain. The dishes were scanned on a flat bed scanner (300 dpi) and the number of colonies and colony diameters were measured using ImageJ.

Cell migration/chemotaxis assays were performed using CytoSelect™ 24-Well Cell Invasion Assay kit (Cell Biolabs Inc., San Diego, CA) essentially as described by the manufacturer. In this assay cell are seeded in transwells with a polycarbonate membrane at the bottom. The membranes are perforated with 8 μm diameter pores and pre-coated with a uniform, 100 micron-thick layer of bovine type I collagen. The transwells are placed in a reservoir containing chemotactic agents and incubated for a time to allow chemotaxis through the membrane. At the endpoint the cells that came completely through the membrane were lysed and Calcein AM florescence measured using fluorometer. In our experiments pCPC or chondrocyte suspensions ($3x10^5$ cells in serum free media) were added to the upper transwell and placed in reservoirs containing serum-free medium with various chemokines, cell lysates, or serum-free medium conditioned by injured explants. The plates were incubated for 24 hours, prior to processing. Cell lysates were transferred to fluorescence plates and read on a SpectraMax M5 multi-detection microplate reader (Molecular Devices Inc., Sunnyvale, CA) set to 485 nm excitation and 538nm emission. Standard curves consisting of known numbers of stained and lysed cells were used to derive cell counts from fluorescence intensity. The data are presented as the percentage of migrating cells (# migrated into the bottom chamber/# seeded in the top chamber X 100) or as a ratio of treated to control. The chemotactic factors used to activate cell migration in this experiment, Stromal cell-derived factor been shown to attract mesenchymal stem cells and progenitor cells (31, 34). CXCL12 and 8 (Invitrogen) were dissolved in culture medium at a concentration of 500 nM. Conditioned medium was made by incubating blunt-impacted explants overnight in 10 ml serum-free medium for 24 hours after impact. The conditioned medium was concentrated 10-fold using Amicon® Ultra centrifugal Filters 10K (Millipore, Billerica, MA). Lysates for testing in the chemotaxis assay were obtained by repeated freeze-thawing of cells from primary cultures of bovine chondrocytes isolated from distal femurs.

Side population assays were performed essentially as described (16).First passage pCPCs and normal chondrocytes in suspension in HBSS ($1 x10^6$/ml) were incubated at 37°C for 1.5 hours with Hoechst-33342 (Sigma) at 2.5 mg/ml with or without verapamil at 5 mM. The cells were washed in cold HBSS and filtered through 70 μm nylon mesh and counterstained with propidium iodide to identify dead cells. Flow cytometric analysis was performed on a Becton Dickinson LSR II with UV (BD Bioscience, San Jose, CA).

The multi-potency of pCPCs was tested by culturing under chondrogenic, osteogenic and adipogenic conditions (44). For chondrogenic differentiation, 1.2 million cells were pelleted and incubated in chondrogenic medium (DMEM containing 10 ng/ml TGF-β1, 0.1 μM dexamethasone, 25 μg/ml L-ascorbate, 100 μg/ml pyruvate, 50 mg/ml ITS+Premix and antibiotics) for 14 days. The pellets were analyzed for proteoglycan-rich matrix formation using Safranin-O/fast green staining of cryosections. To induce osteogenic differentiation, $3x10^4$ trypsinized migrating cells were cultured in osteogenic medium (DMEM/F-12 containing 0.1 μM dexamethasone, 100 mM β-glycerophosphate, 50 μg/ml L-ascorbate and antibiotics) for 14 days and stained with Alizarin Red to detect deposition of calcium phosphate mineralization. We used STEMPRO® Adiopgenesis differentiation kit (GIBCO, Grand Island, NY) to induce adipogenesis. 14 days post-induction, the cells were stained with Oil Red O and imaged on a Nikon XB inverted microscope.

For microarray analysis we isolated RNA from primary cultures of bovine bone marrow stromal cells (BMSCs), from freshly harvested pCPCs, and directly from explant cartilage. BMSCs were isolated from the marrow and subchondral bone of adult bovine tibiae by saline lavage. The lavage was centrifuged and the pelleted cells plated in plastic dishes. After 2 days the dishes were washed to remove non-adherent cells. Adherent cells were allowed to grow for 5 days before harvest. RNA from three batches of cells or cartilage

were pooled for analysis. Cells and cartilage were homogenized in TRIzol® reagent (Invitrogen™ Life Technologies, Carlsbad, CA) and total RNA was extracted using the RNeasy Mini Kit (Qiagen, Valencia, CA) according to the manufacturer's instruction. 50 ng RNA was converted to SPIA amplified cDNA using the Ovation™ RNA Amplification System v2 (NuGEN Technologies, Inc., San Carlos, CA) Biotinylated cDNA was placed onto Bovine Genome Arrays (Affymetrix, Inc., San Carlos, CA),. Arrays were scanned with the Affymetrix Model 3000 scanner and data were collected using the GeneChip operating software (MAS) v5.0.

Real-time PCR was used to compare the expression of stem cell markers in pCPCs and NCs essentially as described (45). Primers were purchased from Integrated DNA Technologies (Coralville, IA). The following primer sequences were used (Forward/Reverse):

1) CD105 CCACTGCCCCAGAGACTGCGC/GCCCCCACAGTGAGTGCTTAGGT
2) CD29 GCGGCCTCCGGGTGGATTCC/GCCGGGAAGGTCCAGGGGC
3) Abcg-2 CCTTGGTTGTCATGGCTTCA/AGTCCTGGGCAGAAGTTTTGTC
4) CD90 CGGTGGTGTTTGGCCATGTAATGA/GAGAGAGGGGAGTCCTATCCTGGT
5) Runx-2 GCATGAAGCCCTATCCAGAGTCT/GCTGATGGAGCTGTTGGTGTAG
6) CD73 AGCTTTCCCAGCCTTCCATGCG/GGGTGTCCTCTTGAGTCCTGCA
7) Sox-9 CGGTGGTGTTTGGCCATGTAATGA/GAGAGAGGGGAGTCCTATCCTGGT
8) CD39 CCCACCCTCTCCTTCCGAGAGG/TGACTGTAACCCTGGAGCTTGGCT
9) FLk-1 TTCCAAGTGGCTAAGGGCAT/TTTAACCACGTTCTTTTCCGACA
10) b-actin TCGACACCGCAACCAGTTCGC/CATGCCGGAGCCGTTGTCGA

The ability of putative progenitor cells to repopulate full-thickness cartilage defects was tested in vitro using bovine osteochondral explants. Full-thickness cartilage defects were created in the center of the explants surfaces using 4-mm biopsy punches. This procedure also resulted in the death of chondrocytes within ~100 microns of the cut edges. After 2-day pre-culture the defects were filled with fibrin hydrogel (Tisseal, Baxter Healthcare Corp., Westlake Village, CA). To assess cartilage matrix formation cryosections through the defects were stained with safranin-O/Fast green after 3 weeks of incubation.

For colony formation assays statistical analysis was performed using SPSS software (Ver.10.0.7, SPSS Inc., Chicago, IL) with a one-way ANOVA and post-hoc pairwise comparison. Flow cytometry data (side population) were evaluated by Students t-test. One-way and Two-way ANOVAs with the Holm-Sidak post-hoc test were used to analyze migration assay data. All the results are expressed as mean ± standard deviation.

Results

Blunt impact-injury to bovine osteochondral explant surfaces caused local chondrocyte death and stimulated the emergence of migratory cells in and around impact sites. These cells began to accumulate 5 days after impact and gradually repopulated previously uninhabited areas (Figure 1A-C). Migrating cells were morphologically distinct from normal chondrocytes in that they were elongated with multiple thin cytoplasmic extensions (Figure 1D). A similar migratory reaction was observed at an impact site in an explanted human talus (Figure 1 D, E) and in a scratch injury (Figure 1 F, G).

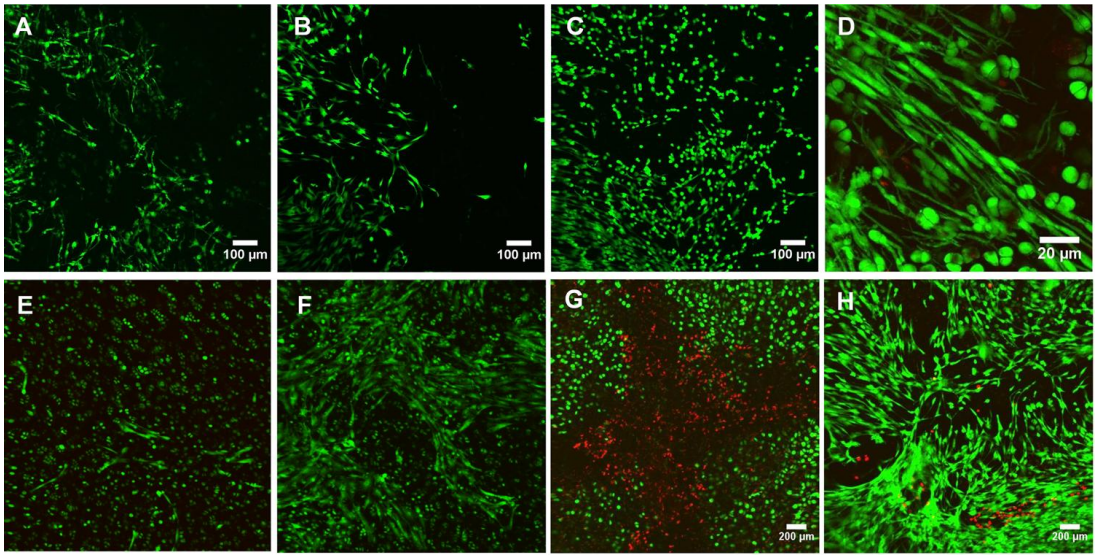

After 5-7 days post-impact surface-adherent migrating cells were detached from the injured explants by trypsin treatment. Some cells were transduced with GFP, and grafted ~4

Figure 1. Repopulation of injured cartilage by migrating cells. (A-C) Confocal images show the same area within an impact site on the surface of a bovine tibial plateau explant stained with calcein AM at 7 days (A), 11 days (B), and 15 days (C) post-impact. The elongated morphology and dendritic appearance of the migrating cells are shown in a high magnification view (D). Confocal images of an impact site on a human talus at 6 days (E) and 10 days (F) post-impact. The images in G and H show dead chondrocytes (red) and live chondrocytes (green) in a bovine explant with a cross-shaped needle scratch. The explant was stained and imaged immediately after the injury (G) and 14 days after injury (H).

mm away from a freshly made impact site on another explant (Figure 2). The number of labeled cells in the impact site increased dramatically from 2-12 days (Figure 2B-D). The clonogenic activity of trypsinized cells was compared with chondrocytes from the upper 1/3 of the cartilage, which included the superficial and transitional zones, and from the bottom 2/3, which included the transitional and deep zones (Figure 3). Chondrocytes were isolated separately from both layers by collagenase-pronase digestion of the matrix. Primary cultures were established and the cells harvested for colony formation assays after 5-7 days in culture. Trypsinized cells in monolayer culture grew more rapidly than chondrocytes (Figure 3A-D). These primary cultures were passaged, seeded in cloning dishes and incubated for 10 days. The dishes were stained with Richardson's dye and the total number of colonies and colony area were measured. Trypsinized cells showed the most vigorous colony formation both in terms of the total

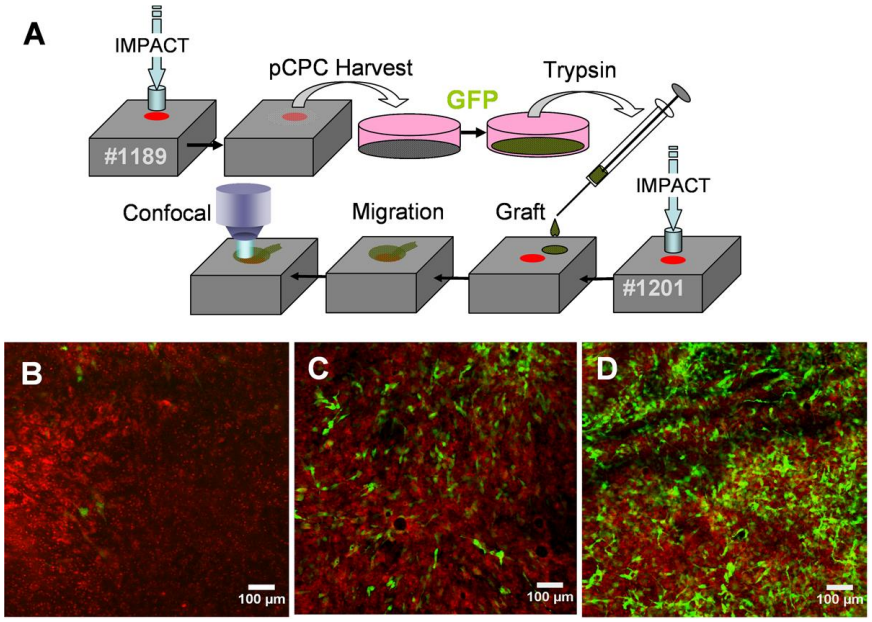

Figure 2. Migration of grafted pCPCs. (A) Procedure for harvesting and grafting pCPCs. The boxes represent two different explants (#1189 and #1201). Explant 1189 was impacted pCPCs were harvested and placed in monolayer culture for GFP transduction. Labeled cells were trypsinized, suspended in a temperature-sensitive hydrogel, and grafted onto explant 1201, which had been impacted a few hours earlier. The impact site was imaged by confocal microscopy at various times after grafting. Grafted GFP-labeled cells (green) can be seen against the background of host cells labeled with a red tracking stain. Exactly the same field within the impact site was imaged at 2 days (B), 5 days (C), and 12 days (D) post-grafting.

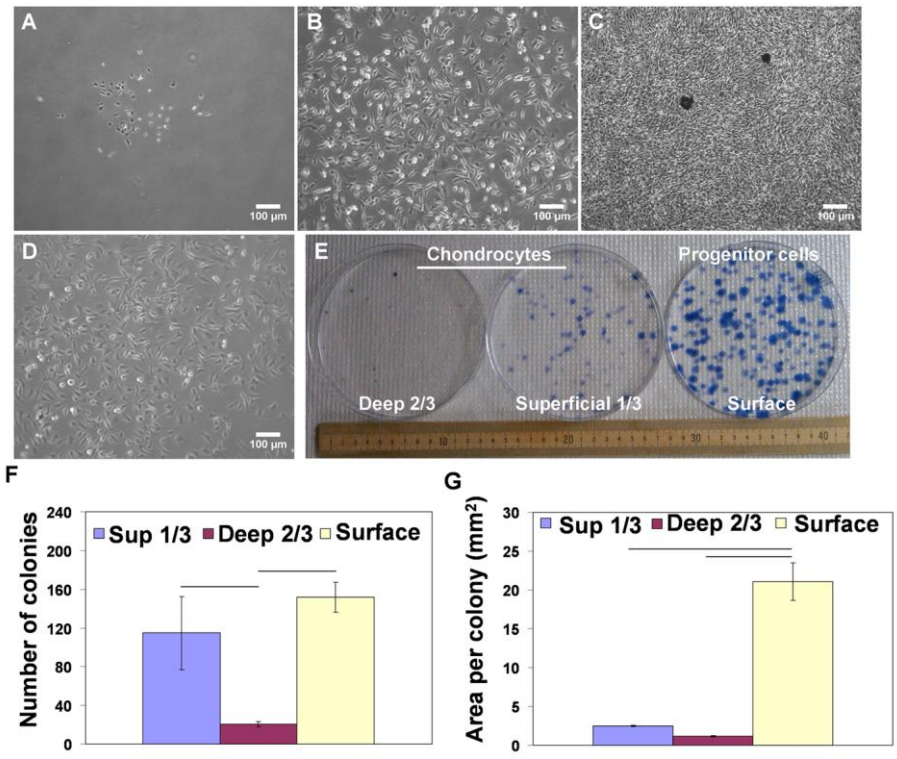

Figure 3. Colony formation by migrating progenitor cells and chondrocytes. (A-D) Light microscope image of single colony of progenitor cells at 2 days (A), 3 days (B), and 6 days (C) after seeding. Image of a chondrocyte colony cultured for 13 days (D). (E) Cloning plates seeded with chondrocytes from the deep and superficial zones or progenitor cells after 10 days of growth. The total number of colonies (F) and average colony area (G) were measured. Crossbars indicate significant differences ($p < 0.05$). Columns and error bars are means and standard deviations based on n=4-5 different batches of cells.

Flow cytometric analysis of Hoechst-stained trypsinized cells and NCs revealed side populations of cells capable of dye exclusion in both populations (Figure 4D). Their numbers in populations of trypsinized cells were significantly greater than in NC populations (0.22 +/- 0.07% versus 0.013 +/- 0.012% respectively, $p = 0.001$). Verapamil treatment reduced side populations to less than 0.005%, indicating that the efflux mechanism depended on the stem cell-associated ABCG transporter. Real-time PCR analysis revealed substantially higher expression of progenitor/stem cell marker genes in pCPCs versus NCs (Figure 4E).

ABCG2 was increased by over 4-fold, Sox-9 by 3.8-fold, and FLK-1 by 2.8. CD105, CD73, CD39, and CD29 were increased by less than 2-fold in pCPCs. However, CD90 was 2-fold higher in NCs than in pCPCs. Microarray analysis showed elevated expression of the progenitor cell markers Notch1 (3.4-fold) and CD44 (4.3-fold) in pCPCs. pCPCs also over-expressed PRG4 by 2.1-fold compared to NCs.

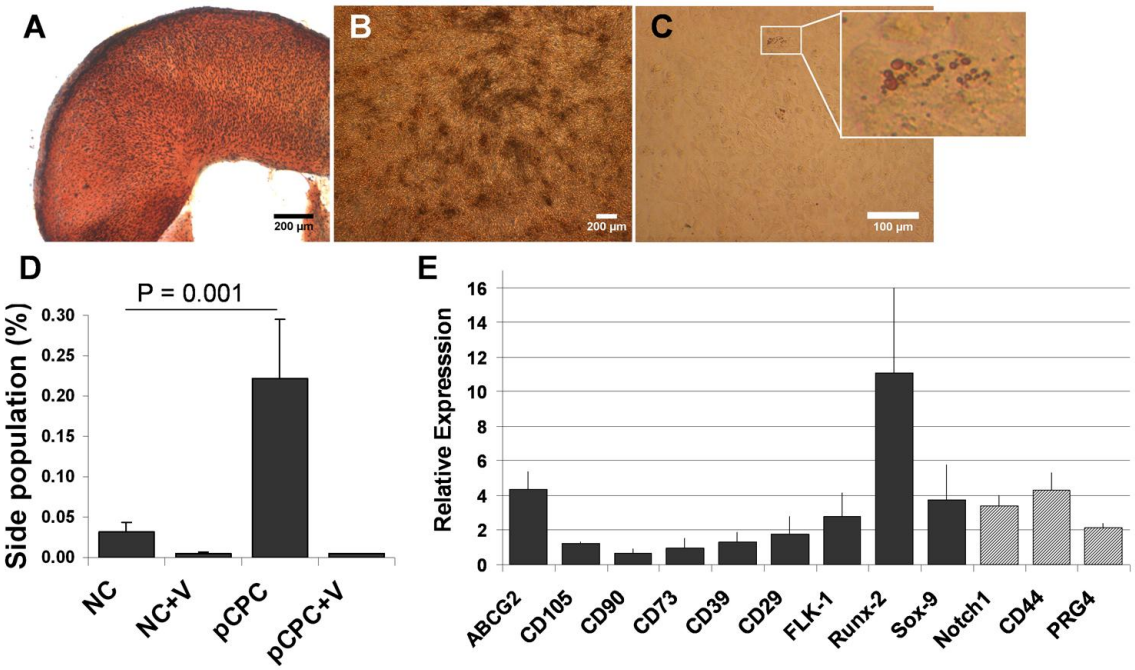

Figure 4. pCPCs show stem cell characteristics (A-C) pCPCs were cultured under chondrogenic (A), osteogenic (B), and adipogenic (C) conditions. The pellet culture showed intense red Safranin-O/fast green staining indicating the presence of cartilage proteoglycans. (B) Deposition of calcium phosphate was detected by staining with Alizarin Red (dark red spots). (C) Only few cells produced positive fat vacuoles in Oil Red O staining. (D) FACS analysis showed that the proportion of SP was significantly higher in progenitor cells than in chondrocytes (p=0.001). As expected Verapamil, an ABCG transport inhibitor, ablated the side population. (E) The graph shows real-time PCR analysis (solid columns) and microarray analysis (hatched columns) of marker gene expression in pCPCs relative to NCs (fold change). For PCR means and standard deviations are based on 3-4 batches of cells from different explants. The microarray data are means and standard deviations based on replicate assays of RNA pooled from three different cell batches.

Two-way analysis of variance revealed that overall, pCPCs were more active *in vitro* chemotaxis assays than NCs (p=0.001), however this depended the chemotactic factor used in the assay (Figure 5A). Compared with untreated control medium CXCL12 significantly increased pCPC chemotaxis (p = 0.003) but had no effect on NCs (p =0.411). In this case, pCPC chemotaxis was significantly higher than NC (p = 0.036). In contrast, neither pCPCs nor NCs responded to CXCL8 (p =0.128 and 0.912 respectively) and the difference between the cell types was not significant (p = 0.109). Conditioned medium from impact-injured explants induced chemotaxis to a similar degree in both pCPCs and NCs (p =0.001). pCPCs were slightly more active than NCs, but the difference was not significant (p = 0.109). Chondrocyte lysates were used to simulate cell death at impact sites. The response to cell lysates was significant for pCPCs and NCs (p =0.001), but the pCPC response was significantly greater than the NC response (p = 0.001). In addition to cell lysates and conditioned medium, pCPCs responded strongly to purified HMGB1 (Figure 5B). HMGB1 at 10 or 20 nM significantly enhanced chemotaxis compared with controls (p = 0.001). These effects and the effects of cell lysates were suppressed and by an antibody to the AGE receptor: values from lysates + anti-RAGE or 10 nm HMGB1 + RAGE were not significantly higher than control (p = 0.058 and 0.075 respectively). Immunoblots confirmed the presence of HMGB1 in cell lysates and conditioned medium (Figure 5C).

Gene expression microarrays showed substantial phenotypic differences among pCPCs and NCs and between BMSCs and NCs. This was well illustrated by the lengthy list of genes whose expression varied by more than 5-fold (Table). In general, migration and growth-related genes were expressed at higher levels in MSCs and pCPCs than in NCs. Chemokines involved in stem and progenitor cell chemotaxis (35, 46) were strikingly up-regulated in pCPCs versus NCs. CXCL2, CXCL5, and CXCL12 (stromal cell derived factor-1) mRNA levels were more than 10 times greater in pCPCs than in NCs, while CXCL8 was increased by 41-fold. MSCs also showed increased CXC12 expression compared with NCs (27-fold increase), but other chemokines were not elevated. Doublecortin-like kinase 1 (DCLK), a regulator of microtubule polymerization in cell migration was elevated by 9-fold and 24-fold over NCs in pCPCs and MSCs respectively. Matrix protease expression was also greatly enhanced in pCPCs and NCs: Compared with NCs, pCPCs and MSCs expressed 7-fold to 12-fold higher levels of the matrix peptidase ADAMTS-1 and -4, and 126-150-fold lower levels of the serine peptidase inhibitor SERPINA1. Genes involved in cell division including Aurora kinases A and B and cyclin B were expressed at 4-12-fold higher levels in pCPCs and MSCs versus NCs.

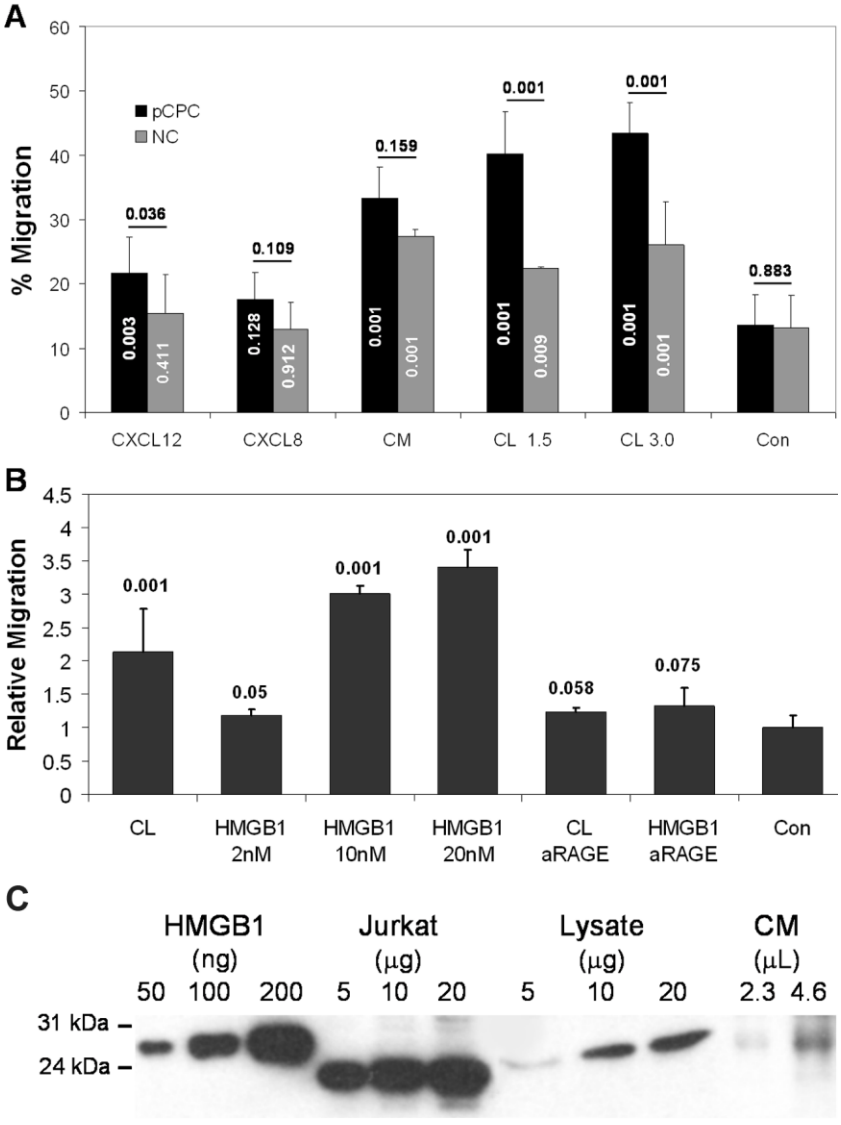

Figure 5. Chemotactic activity. (A) the percentages of pCPCs and NCs that responded to chemokines (CXCL12 and CXCL8), conditioned medium from injured explants (CM), and cell lysates (CL) made from 1.5 x 10^5 cells (1.5) and 3.0 x 10^6 cells (3.0). Naïve medium was used as a control (Con). The numbers above the bars indicate p values for differences between pCPC and NC. Numbers within the columns are p values for differences between treatments and control. (B) The graph shows pCPC chemotaxis in response to cell lysates and to purified HMGB1 at the indicated concentrations. The effects of a RAGE blocking antibody (aRAGE) on responses to HMGB1 (10 nM) or lysates (3.0 x 10^5 cells) were also tested. Values were normalized to control. Columns and error bars are means and standard deviations (n = 3-9). The numbers above the columns indicate p values for treated versus control (one-way ANOVA). (C) A western blot confirmed the presence of HMGB1 (~ 25 kDa) in the chondrocyte lysates and conditioned medium used for chemotaxis assays. Purified HMGB1 and Jurkat cell lysates were included as positive controls. The amounts of protein (μg) or volume of conditioned medium (μL) loaded in each lane were as indicated.

Large numbers of pCPCs were found in fibrin-filled defects after 3 weeks in culture. They produced a cartilage like matrix with strong staining for proteoglycans. (Figure. 6).

Gene	Description	I.D.	Fold Change		
			pCPC/NC	BMSC/NC	BMSC/pCPC
ITGA5	integrin, alpha 5	NM_001166500	**5.6**	3.9	-1.5
RND3	Rho family GTPase 3	NM_001099104	**6.0**	11.6	1.9
ADAMTS1	ADAM metallopeptidase with thrombospondin 1	NM_001101080	**6.8**	11.0	1.6
CCL5	chemokine (C-C motif) ligand 5	NM_175827	**7.7**	-2.1	-16.0
AURKB	aurora kinase B	NM_183084	**7.8**	4.9	-1.6
RACGAP1	Rac GTPase activating protein 1	XM_592496	**8.0**	4.8	-1.7
HMMR	hyaluronan-mediated motility receptor	XM_590028	**8.3**	3.3	-2.5
WNT10B	wingless member 10B	XM_586498	**8.3**	41.1	4.9
ADAMTS4	ADAM metallopeptidase with thrombospondin 4	NM_181667	**8.5**	2.3	-3.8
DCLK1	doublecortin-like kinase 1	NM_001109962	**9.1**	19.1	2.1
AURKA	aurora kinase A	NM_001038028	**9.8**	4.5	-2.3
PLAT	plasminogen activator, tissue	NM_174146	**10.4**	2.0	-5.2
PLAU	plasminogen activator, urokinase	NM_174147	**11.6**	22.3	2.0
CXCL5	chemokine (C-X-C motif) ligand 5	NM_174300	**14.2**	11.4	-1.2
CCNB1	cyclin B1	NM_001045872	**14.8**	9.1	-1.6
IL6	interleukin 6 (interferon, beta 2)	NM_173923	**15.5**	1.3	19.9
CCNB2	cyclin B2	NM_174264	**15.6**	5.1	-3.1
CXCL2	chemokine (C-X-C motif) ligand 2	NM_175700	**18.2**	-1.6	-24.6
CD83	CD83 molecule	NM_001046590	**20.6**	5.1	-4.1
CXCL8	interleukin 8	NM_173925	**20.6**	5.1	-4.1
CXCL12	chemokine (C-X-C motif) ligand 12	NM_001113174	**28.1**	27.4	-0.1
DOCK10	dedicator of cytokinesis 10	XM_001787477	**32.4**	67.9	2.1
CDH2	cadherin 2, type 1, N-cadherin (neuronal)	NM_001166492	**67.8**	165.3	2.4
COL9A1	collagen type IX, alpha1	XM_601325	**-5.5**	-5.4	0.0
FGFRL1	fibroblast growth factor receptor-like 1	XM_610839	**-5.6**	-10.8	-2.0
INSR	insulin receptor	XM_590552	**-5.6**	-6.0	-1.1
TIMP4	TIMP metallopeptidase inhibitor 4	NM_001045871	**-6.1**	-5.7	1.1
ACAN	aggrecan	NM_173981	**-10.1**	-23.6	-18.7
FZD9	frizzled homolog 9 (Drosophila)	XM_599625	**-12.3**	-14.1	-1.1
COL2	collagen type II alpha 1	NM_001001135	**-11.2**	-19.1	-1.0
COL9A2	collagen type IX, alpha2	XM_582312	**-41.0**	-73.7	-1.8
COL10A1	collagen, type X, alpha 1	NM_174634	**-42.6**	-42.6	1.0
FRZB	frizzled-related protein	NM_174059	**-112.3**	-96.1	1.2
COMP	cartilage oligomeric matrix protein	NM_001166517	**-125.6**	-116.8	1.1
CHAD	chondroadherin	NM_174019	**-130.3**	-109.9	1.2
SERPINA1	serpin peptidase inhibitor, clade A	NM_173882	**-150.3**	-135.0	0.1

Table 1. Gene expression in pCPCs versus NCs and BMSCs. Values represent genes expressed in pCPCs that were at least 5-fold lower or higher than in NCs. Many of the most highly over- or under-expressed genes function in proliferation and chemotaxis.

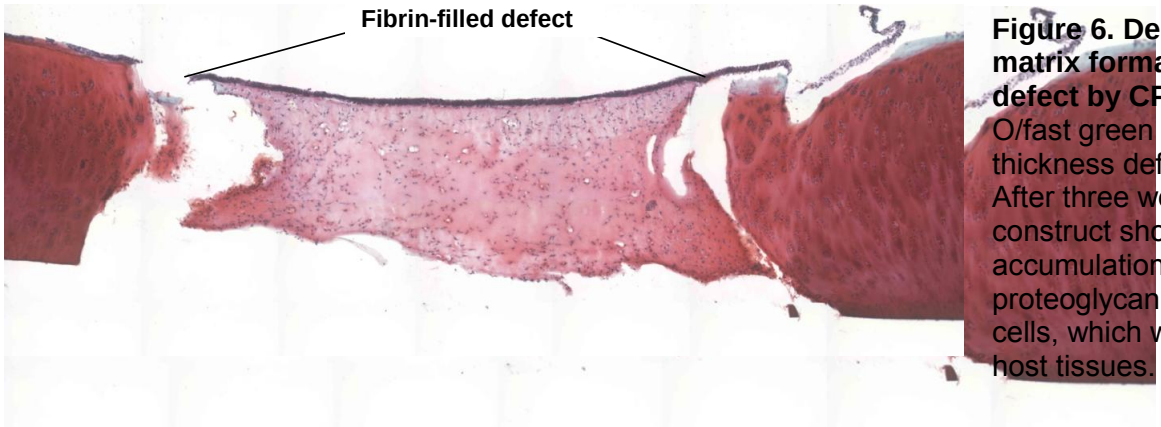

Figure 6. De novo cartilage matrix formation in a chondral defect by CPCs. Safranin-O/fast green stain in a full-thickness defect injury explant. After three weeks, the fibrin construct showed the accumulation of abundant proteoglycan by progenitor-like cells, which were migrated from host tissues.

Discussion

The results of these experiments demonstrate that the migrating cells we observed on injured bovine osteochondral explants closely resemble chondrogenic progenitors previously identified in normal and osteoarthritic human cartilage (7, 15, 17, 23, 25). The cells' chemotactic activity, clonogenicity, limited multipotency, and side population were all notably consistent with published descriptions of progenitor cells from cartilage and other tissues. Gene expression microarrays and real-time PCR showed that pCPCs also over-expressed stem/progenitor-associated genes compared to NCs. Although the origin of pCPCs is still unclear, their initial appearance on cartilage surfaces in our isolated explant model and the need for cartilage injury to provoke this response strongly suggest that the cells came from the cartilage matrix itself. Cells from the top 1/3 of the cartilage matrix were significantly more clonogenic than cells from the bottom 2/3 of the matrix, suggesting that pCPCs were more abundant in the superficial/transitional zones.

Live imaging studies revealed the emergence of elongated cells with multiple filopodia onto the surfaces of explants their migration toward of blunt impact sites. Grafted GFP-labeled pCPCs. Imaging studies of an injured human explant showed a similar response to impact injury, indicating that our observations were not unique to the bovine system. Moreover, a scratch injury that caused local chondrocyte death resulted in the same response as impact injury, suggesting a generalized response to cell and tissue damage that does not depend on the mode of injury.

In vitro assays confirmed that medium conditioned by impacted cartilage or whole cell lysates were relatively strong chemoattractants for pCPCs. These data suggested that pCPC migration to impacted cartilage is driven, at least in part, by dead cell debris, which contains a number of homing factors that draw stem and immune cells to injured tissues (47-49). Further study implicated the nuclear protein HMGB1 as the primary chemoattractant in our system. A blocking antibody to the RAGE receptor diminished migration, suggesting that HMGB1 effects were mediated partly by RAGE. pCPCs themselves also substantially over-expressed multiple chemokines i
ncluding CXCL12. Moreover, expression of CXCR7, a CXCL12 receptor, was
elevated in pCPCs, suggesting autocrine/paracrine induction of chemotaxis. This would likely amplify progenitor cell recruitment to injured cartilage and might continue to promote chemotaxis even after cell debris is cleared. pCPCs were able to migrate through collagen and fibrin matrices with relative ease, suggesting high matrix protease activity. Interestingly, gene expression profiling identified matrix proteinases (plasminogen activator, cathepsin C, ADAMT-1, -4) as among the most highly up-regulated genes and proteinase inhibitors (TIMP 4, SERPIN A1) as among the most highly down-regulated genes in pCPCs. These differences were consistent with the increased invasive behavior of pCPCs compared with NCs. Migration-related genes (DCLK, Rac and Rho GTPases, RHAMM) were also relatively over-expressed by pCPCs compared to NCs. Many of the same genes were regulated similarly in BMSCs, which are known for their migratory capability.

The rapid accumulation of hundreds of pCPCs at injury sites on explant surfaces was unlikely to be due to migration alone, as that would have noticeably depopulated the surrounding matrix. Rapid proliferation on the cartilage surface is a much more likely explanation. This notion was corroborated by clonogenic assay data, which showed that pCPCs formed significantly larger colonies than NCs from either the deep or superficial zones, a clear indication of a faster growth rate. Gene expression data showing large relative increases (versus NCs) in mRNAs for cyclins b1 and b2 and other proliferation-related genes (e.g. aurora kinases, DOCK10) were consistent with a highly proliferative phenotype. Expression levels for these genes in MSCs, which are also noted for rapid proliferation, were similar to pCPCs . However, pCPCs also clearly shared many features with NCs including their similarity in PRG4 expression, a nominal marker of superficial zone chondrocytes.

The multi-potency of pCPCs was tested in conventional culture systems. We found that with appropriate stimulation they readily formed cartilaginous or boney matrices, but were unresponsive to adipogenic conditions: less than 1% stained with oil red O compared with more than 14% of bone marrow derived MSCs. This was consistent with the findings of Grogan *et al*., who showed that CPCs isolated from OA cartilage also failed to trans-differentiate into adipocytes (15). These results and the low numbers of side population cells identified by flow cytometric analysis indicate that 2% or less of the pCPC population were true stem cells, on par with published data on CPCs (16).

Safranin-O histology showed cells that invaded the fibrin filler deposited a proteoglycan-rich pericellular matrix. This signature chondrogenic activity involves coordinated expression of numerous structural proteins (e.g. aggrecan, hyaluronan, collagens, fibronectin) and processing enzymes (e.g. MMPs, lysyl oxidase, prolyl hydroylase) (refs). Staining immediately around the cells (50-100 microns) was often as intense as in normal cartilage matrix, but in only 1 of 4 cases did the entire fibrin structure contain normal proteoglycan levels. On

the other hand, the DNA content of the fibrin gels was modestly greater than normal cartilage, an indication of near normal cellularity. It remains to be seen if all of these cells will eventually engage in high levels of matrix production spontaneously, or will require intervention with chondrogenic growth factors, which we saw drive 90% of pCPCs in pellet cultures to vigorously synthesize proteoglycans.

Based on our results, CPCs may also be harvested to serve as a source for cell implantation. However, the main appeal of a CPC-based strategy lies in the cell's ability to heal by self-congregating at injury sites, thereby eliminating the costs and risks associated with ex vivo cell expansion and the additional surgery needed for grafting. The identification of chemotactic factors like HMGB1 could lead to methods to augment CPC homing, increasing their potential for repair.

KEY RESEARCH ACCOMPLISHMENTS: Bulleted list of key research accomplishments emanating from this research.

- Injury-responsive migrating cells are chondrogenic progenitors
- Identification of cell-death related chemotactic factors that recruit progenitors to injured tissue
- In situ cartilage repair by chondrogenic progenitors using a fibrin scaffold

REPORTABLE OUTCOMES:

Abstracts

1. McCabe D, Seol D, Choe H, Stroud, N, Buckwalter J, Martin J. Do Cartilage-derived Stem Cells Repopulate Dead Zones in Injured Cartilage? Trans Ortho Res Soc 35; 2511, 2010
2. Zheng H, Lehman A, Laughlin A, Buckwalter JA, Martin JA. "Chondrogenic Potential of Mesenchymal Progenitor Cells (MPCs) from Different Connective Tissues" Poster # 1729.
3. Brouillette M, Wagner V, Martin JA, Ramakrishnan P. "Static Mechanical Stress Increases Oxidant Production in Cartilage Explant" Poster # 2179
4. Choe H, Seol D, Lehman A, Heiner A, Ramakrishnan P,Lim T, Martin JA. "Effect of Chemokines on Migratory Progenitor Cell (MPC) Migration" Poster # 1772
5. Jang K, Seol D, Ramakrishnan P, Lehman A, Dove E, Lim T, Martin JA. "Effect of Low-Intensity Pulsed Ultrasound (LIPUS) on Cartilage Healing; A Preliminary Study" Poster # 2097
6. Journot B, Walter M, Martin JA. "A Novel System to Automate Image Processing and Analysis for Cell Microscopy" Poster #1593
7. McCabe D, Lehman A, Amendola J, Walter M, Buckwalter J, Martin JA. "Characterization of a Stem Cell-Like Population in Cartilage" Poster #2059
8. Sauter E, Lehman A, McKinley TO, Martin JA. Title: "Effects of Cytoskeletal Inhibitors on Reactive Oxygen Species and Viability in Chondrocytes Following Blunt Impact Injury to Osteochondral Explants" Poster #2165
9. Reese ER, Sauter EE, Heiner AD, Stroud NJ, Martin JA, Mckinley TO. Kinetics of Reactive Oxygen Species Production by Chondrocytes Following Blunt Impact Injury to Osteochondral Explants Trans Ortho Res Soc 35; 1731, 2010

Manuscripts

Dongrim Seol, Daniel J. McCabe, Hyeonghun Choe, Hongjun Zheng, Keewoong Jang, Morgan W. Walter, Yin Yu, Abigail D. Lehman1, Prem S. Ramakrishnan, Lei Ding, Joseph A. Buckwalter, James A. Martin Chondrogenic Progenitor Cells Respond to Cartilage Injury. (2011) Arth. Rheum. (submitted)

Proposals

September 2011. Department of Veterans Affairs Medical Center. *Induction of chondrogenic progenitor cells for cartilage repair.* Joseph A. Buckwalter P.I

Students.

August 201. Dongrim Seol, Ph.D thesis *Migrating cell response to cartilage injury*. Mentor: James Martin

CONCLUSION: The results confirmed the presence of potentially reparative chondrogenic progenitors in articular cartilage and demonstrated a chemotactic mechanism that may be used to attract them to injury sites. Moreover, we showed that providing a fibrin matrix enabled progenitors to regenerate a cartilage matrix in chondral defects. We are now in a position to tests the efficacy of this system for the repair of chondral defects in vivo as described in our recent proposal to the Veterans Administration.

REFERENCES:

1. Buckwalter JA, Brown TD. Joint injury, repair, and remodeling: roles in post-traumatic osteoarthritis. Clin Orthop Relat Res 2004(423):7-16.
2. Marsh JL, Borrelli J, Jr., Dirschl DR, Sirkin MS. Fractures of the tibial plafond. Instr Course Lect 2007;56:331-52.
3. Marsh JL, Weigel DP, Dirschl DR. Tibial plafond fractures. How do these ankles function over time? J Bone Joint Surg Am 2003;85-A(2):287-95.
4. Hunziker EB. The elusive path to cartilage regeneration. Adv Mater 2009;21(32-33):3419-24.
5. Gillogly SD, Myers TH, Reinold MM. Treatment of full-thickness chondral defects in the knee with autologous chondrocyte implantation. J Orthop Sports Phys Ther 2006;36(10):751-64.
6. Simon TM, Jackson DW. Articular cartilage: injury pathways and treatment options. Sports Med Arthrosc 2006;14(3):146-54.
7. Williams RJ, 3rd, Harnly HW. Microfracture: indications, technique, and results. Instr Course Lect 2007;56:419-28.
8. Yen YM, Cascio B, O'Brien L, Stalzer S, Millett PJ, Steadman JR. Treatment of osteoarthritis of the knee with microfracture and rehabilitation. Med Sci Sports Exerc 2008;40(2):200-5.
9. Bedi A, Feeley BT, Williams RJ, 3rd. Management of articular cartilage defects of the knee. J Bone Joint Surg Am;92(4):994-1009.
10. Bekkers JE, Inklaar M, Saris DB. Treatment selection in articular cartilage lesions of the knee: a systematic review. Am J Sports Med 2009;37 Suppl 1:148S-55S.
11. Safran MR, Seiber K. The evidence for surgical repair of articular cartilage in the knee. J Am Acad Orthop Surg;18(5):259-66.
12. Dorotka R, Windberger U, Macfelda K, Bindreiter U, Toma C, Nehrer S. Repair of articular cartilage defects treated by microfracture and a three-dimensional collagen matrix. Biomaterials 2005;26(17):3617-29.
13. Breinan HA, Hsu HP, Spector M. Chondral defects in animal models: effects of selected repair procedures in canines. Clin Orthop Relat Res 2001(391 Suppl):S219-30.
14. Dowthwaite GP, Bishop JC, Redman SN, Khan IM, Rooney P, Evans DJ, et al. The surface of articular cartilage contains a progenitor cell population. J Cell Sci 2004;117(Pt 6):889-97.
15. Grogan SP, Miyaki S, Asahara H, D'Lima DD, Lotz MK. Mesenchymal progenitor cell markers in human articular cartilage: normal distribution and changes in osteoarthritis. Arthritis Res Ther 2009;11(3):R85.
16. Hattori S, Oxford C, Reddi AH. Identification of superficial zone articular chondrocyte stem/progenitor cells. Biochem Biophys Res Commun 2007;358(1):99-103.
17. Khan IM, Williams R, Archer CW. One flew over the progenitor's nest: migratory cells find a home in osteoarthritic cartilage. Cell Stem Cell 2009;4(4):282-4.
18. Hilfiker A, Kasper C, Hass R, Haverich A. Mesenchymal stem cells and progenitor cells in connective tissue engineering and regenerative medicine: is there a future for transplantation? Langenbecks Arch Surg;396(4):489-97.
19. Pittenger MF, Mackay AM, Beck SC, Jaiswal RK, Douglas R, Mosca JD, et al. Multilineage potential of adult human mesenchymal stem cells. Science 1999;284(5411):143-7.
20. Prockop DJ. Repair of tissues by adult stem/progenitor cells (MSCs): controversies, myths, and changing paradigms. Mol Ther 2009;17(6):939-46.
21. Quesenberry PJ, Colvin G, Dooner G, Dooner M, Aliotta JM, Johnson K. The stem cell continuum: cell cycle, injury, and phenotype lability. Ann N Y Acad Sci 2007;1106:20-9.
22. Spees JL, Whitney MJ, Sullivan DE, Lasky JA, Laboy M, Ylostalo J, et al. Bone marrow progenitor cells contribute to repair and remodeling of the lung and heart in a rat model of progressive pulmonary hypertension. FASEB J 2008;22(4):1226-36.
23. Alsalameh S, Amin R, Gemba T, Lotz M. Identification of mesenchymal progenitor cells in normal and osteoarthritic human articular cartilage. Arthritis Rheum 2004;50(5):1522-32.
24. Golebiewska A, Brons NH, Bjerkvig R, Niclou SP. Critical appraisal of the side population assay in stem cell and cancer stem cell research. Cell Stem Cell;8(2):136-47.
25. Koelling S, Kruegel J, Irmer M, Path JR, Sadowski B, Miro X, et al. Migratory chondrogenic progenitor cells from repair tissue during the later stages of human osteoarthritis. Cell Stem Cell 2009;4(4):324-35.
26. Klune JR, Dhupar R, Cardinal J, Billiar TR, Tsung A. HMGB1: endogenous danger signaling. Mol Med 2008;14(7-8):476-84.
27. Zhang Q, O'Hearn S, Kavalukas SL, Barbul A. Role of High Mobility Group Box 1 (HMGB1) in Wound Healing. J Surg Res.

28. Jeannin P, Jaillon S, Delneste Y. Pattern recognition receptors in the immune response against dying cells. Curr Opin Immunol 2008;20(5):530-7.
29. Foell D, Wittkowski H, Roth J. Mechanisms of disease: a 'DAMP' view of inflammatory arthritis. Nat Clin Pract Rheumatol 2007;3(7):382-90.
30. Meng E, Guo Z, Wang H, Jin J, Wang J, Wang H, et al. High mobility group box 1 protein inhibits the proliferation of human mesenchymal stem cells and promotes their migration and differentiation along osteoblastic pathway. Stem Cells Dev 2008;17(4):805-13.
31. Stich S, Loch A, Leinhase I, Neumann K, Kaps C, Sittinger M, et al. Human periosteum-derived progenitor cells express distinct chemokine receptors and migrate upon stimulation with CCL2, CCL25, CXCL8, CXCL12, and CXCL13. Eur J Cell Biol 2008;87(6):365-76.
32. Chavakis E, Urbich C, Dimmeler S. Homing and engraftment of progenitor cells: a prerequisite for cell therapy. J Mol Cell Cardiol 2008;45(4):514-22.
33. Palumbo R, Galvez BG, Pusterla T, De Marchis F, Cossu G, Marcu KB, et al. Cells migrating to sites of tissue damage in response to the danger signal HMGB1 require NF-kappaB activation. J Cell Biol 2007;179(1):33-40.
34. Kitaori T, Ito H, Schwarz EM, Tsutsumi R, Yoshitomi H, Oishi S, et al. Stromal cell-derived factor 1/CXCR4 signaling is critical for the recruitment of mesenchymal stem cells to the fracture site during skeletal repair in a mouse model. Arthritis Rheum 2009;60(3):813-23.
35. Kucia M, Jankowski K, Reca R, Wysoczynski M, Bandura L, Allendorf DJ, et al. CXCR4-SDF-1 signalling, locomotion, chemotaxis and adhesion. J Mol Histol 2004;35(3):233-45.
36. Carter DR, Beaupre GS, Wong M, Smith RL, Andriacchi TP, Schurman DJ. The mechanobiology of articular cartilage development and degeneration. Clin Orthop Relat Res 2004(427 Suppl):S69-77.
37. Duda GN, Eilers M, Loh L, Hoffman JE, Kaab M, Schaser K. Chondrocyte death precedes structural damage in blunt impact trauma. Clin Orthop Relat Res 2001(393):302-9.
38. Isaac DI, Meyer EG, Haut RC. Chondrocyte damage and contact pressures following impact on the rabbit tibiofemoral joint. J Biomech Eng 2008;130(4):041018.
39. Phillips DM, Haut RC. The use of a non-ionic surfactant (P188) to save chondrocytes from necrosis following impact loading of chondral explants. J Orthop Res 2004;22(5):1135-42.
40. Rundell SA, Baars DC, Phillips DM, Haut RC. The limitation of acute necrosis in retro-patellar cartilage after a severe blunt impact to the in vivo rabbit patello-femoral joint. J Orthop Res 2005;23(6):1363-9.
41. Beecher BR, Martin JA, Pedersen DR, Heiner AD, Buckwalter JA. Antioxidants block cyclic loading induced chondrocyte death. Iowa Orthop J 2007;27:1-8.
42. Martin JA, McCabe D, Walter M, Buckwalter JA, McKinley TO. N-acetylcysteine inhibits post-impact chondrocyte death in osteochondral explants. J Bone Joint Surg Am 2009;91(8):1890-7.
43. Goodwin W, McCabe D, Sauter E, Reese E, Walter M, Buckwalter JA, et al. Rotenone prevents impact-induced chondrocyte death. J Orthop Res 2010;28(8):1057-63.
44. Jiang Y, Jahagirdar BN, Reinhardt RL, Schwartz RE, Keene CD, Ortiz-Gonzalez XR, et al. Pluripotency of mesenchymal stem cells derived from adult marrow. Nature 2002;418(6893):41-9.
45. Seol D, Choe H, Zheng H, Jang K, Ramakrishnan PS, Lim TH, et al. Selection of reference genes for normalization of quantitative real-time PCR in organ culture of the rat and rabbit intervertebral disc. BMC Res Notes 2011;4:162.
46. Kucia M, Reca R, Miekus K, Wanzeck J, Wojakowski W, Janowska-Wieczorek A, et al. Trafficking of normal stem cells and metastasis of cancer stem cells involve similar mechanisms: pivotal role of the SDF-1-CXCR4 axis. Stem Cells 2005;23(7):879-94.
47. Harris HE, Raucci A. Alarmin(g) news about danger: workshop on innate danger signals and HMGB1. EMBO Rep 2006;7(8):774-8.
48. Gauley J, Pisetsky DS. The translocation of HMGB1 during cell activation and cell death. Autoimmunity 2009;42(4):299-301.
49. Hreggvidsdottir HS, Ostberg T, Wahamaa H, Schierbeck H, Aveberger AC, Klevenvall L, et al. The alarmin HMGB1 acts in synergy with endogenous and exogenous danger signals to promote inflammation. J Leukoc Biol 2009;86(3):655-62.